Coupling ray theory for S waves

Petr Bulant * & Luděk Klimeš, Department of Geophysics, Faculty of Mathematics and Physics, Charles University, Prague, Czech Republic, http://sw3d.mff.cuni.cz/staff/bulant.htm, http://sw3d.mff.cuni.cz/staff/klimes.htm

Summary

The coupling ray theory provides a continuous transition between the isotropic and anisotropic ray theories, and is particularly important at degrees of anisotropy and frequencies typical in seismic exploration and structural seismology on all scales. In this paper, isotropic–ray–theory, coupling–ray–theory, and anisotropic–ray–theory seismograms in a realistic weakly anisotropic model are compared. The most pronounced differences can be observed in polarization. Then, the coupling–ray–theory seismograms in four models of differing anisotropy are compared. For weaker anisotropy, just the polarization changes with increasing anisotropy. If anisotropy is increased further, the clear development of S–wave splitting can be observed.

Coupling ray theory for S waves

Traditionally, there are two different high-frequency asymptotic ray theories: the *isotropic ray theory* assuming equal velocities of both S waves, and the *anisotropic ray theory* assuming both S waves strictly decoupled. In the isotropic ray theory, the S–wave polarization vectors do not rotate about the ray, whereas in the anisotropic ray theory they may rotate rapidly about the ray, see Figure 1. Thomson, Kendall & Guest (1992) demonstrated analytically that the high–frequency asymptotic error of the anisotropic ray theory is inversely proportional to the square root or higher–order root of the frequency if a ray passes through the point of equal S–wave eigenvalues of the Christoffel matrix.

In weakly anisotropic models, at moderate frequencies, the S–wave polarization vector tends to remain unrotated about the ray, but is partly attracted by the rotation of the eigenvectors of the Christoffel matrix. The intensity of the attraction increases with frequency. This behaviour of the S–wave polarization vector is described by the *coupling ray theory* proposed by Coates & Chapman (1990) and (in the quasi–isotropic approximation) by Pšenčík (1998). The coupling ray theory is applicable at all degrees of anisotropy, from isotropic models to considerably anisotropic ones. The frequency–dependent coupling ray theory is the generalization of both the zero–order isotropic and anisotropic ray theories and provides continuous transition between them. The numerical algorithm for calculating the frequency–dependent complex–valued S–wave polarization vectors of the coupling ray theory has been designed by Bulant & Klimeš (2002), and the accuracy of the algorithm has been estimated. The estimate enables the integration step to be controlled, so that the relative error in the wavefield amplitudes due to the integration is kept below a given limit, which is of principal importance for numerical applications.

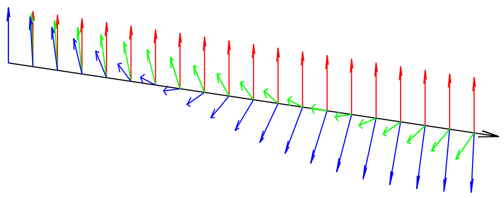

Figure 1. S–wave polarization vector along a ray: Isotropic ray theory polarization vector ($\omega = 0$); Coupling ray theory polarization vector ($0 < \omega < \infty$); Anisotropic ray theory polarization vector ($\omega = \infty$).

Numerical examples

The vertically heterogeneous 1–D anisotropic model QI was used by Pšenčík & Dellinger (2001, model WA rotated by 45°) for comparison of the coupling–ray–theory synthetic seismograms with the reflectivity method. The density–normalized elastic moduli a_{ijkl} in both model QI and in the reference isotropic model QI0 are interpolated linearly with depth. For the discussion and description of this model refer to Pšenčík & Dellinger (2001).

The differences of the elastic moduli of model QIH from the elastic moduli of the reference isotropic model QI0 are exactly twice smaller than the differences of model QI. The differences of the elastic moduli of model QI2 from the elastic moduli of the reference isotropic model QI0 are exactly twice larger than the differences of model QI. The differences of the elastic moduli of model QI4 from the elastic moduli of the reference isotropic model QI0 are exactly 4 times larger than the differences of model QI. For a description of models QI0, QI, QI2 and QI4 refer to Klimeš & Bulant (2004; 2006).

The synthetic seismograms were calculated at 29 receivers located in a vertical well drilled 1 km from a vertical force, see Figure 2. The source time function is the Gabor signal with reference frequency 50 Hz, band–pass filtered by a cosine filter.

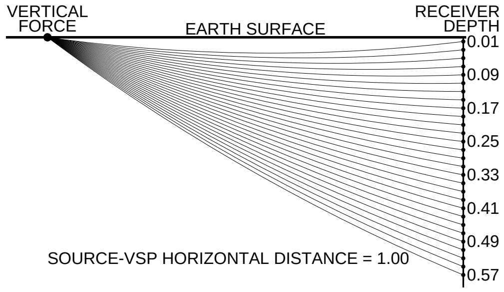

Figure 2. The source and receiver configuration in models QI*.

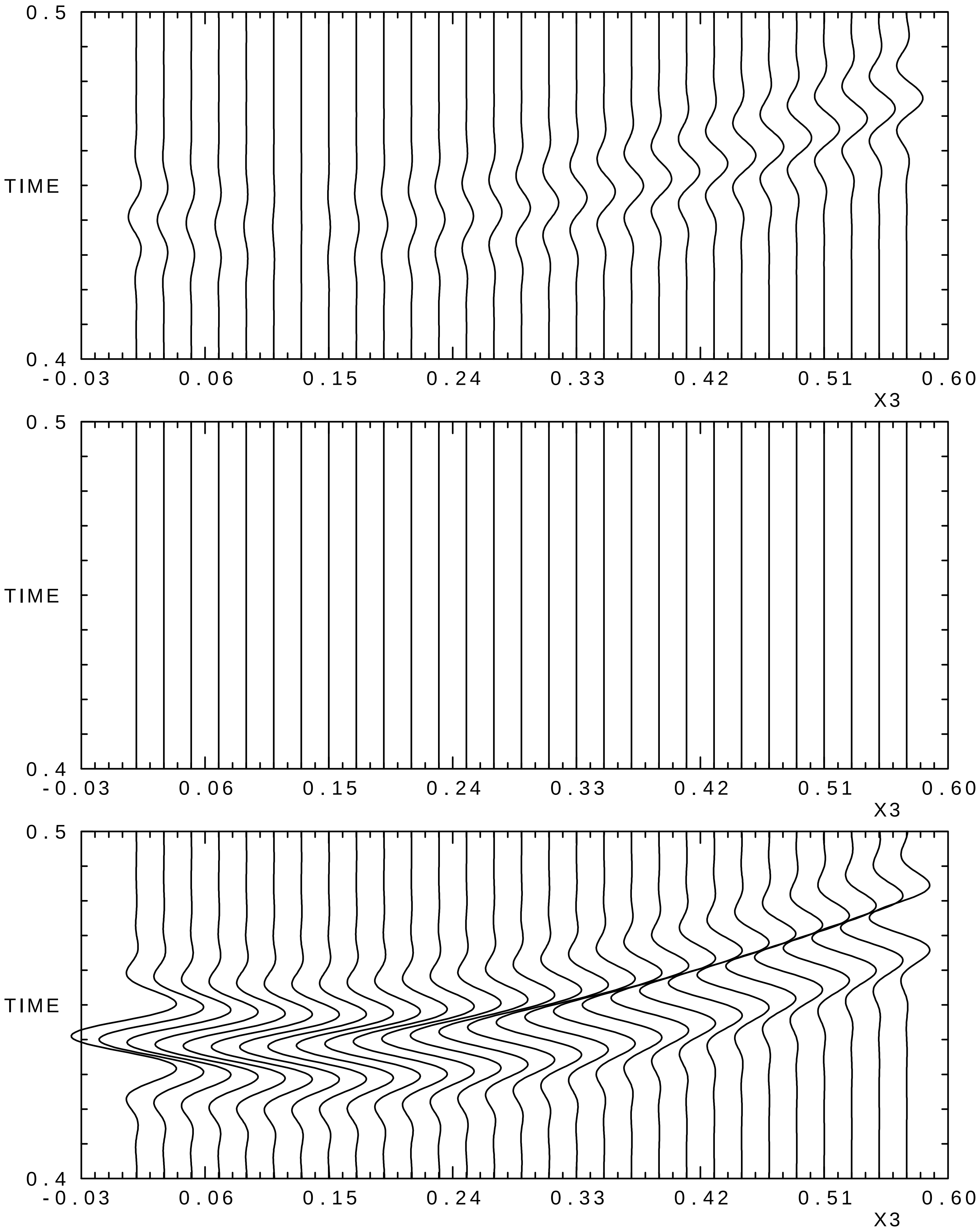

Figure 3. Isotropic–ray–theory seismograms in model QIH (actually calculated in isotropic model QI0). From top to bottom: the first (radial) component, the second (transverse) component, the third (vertical) component.

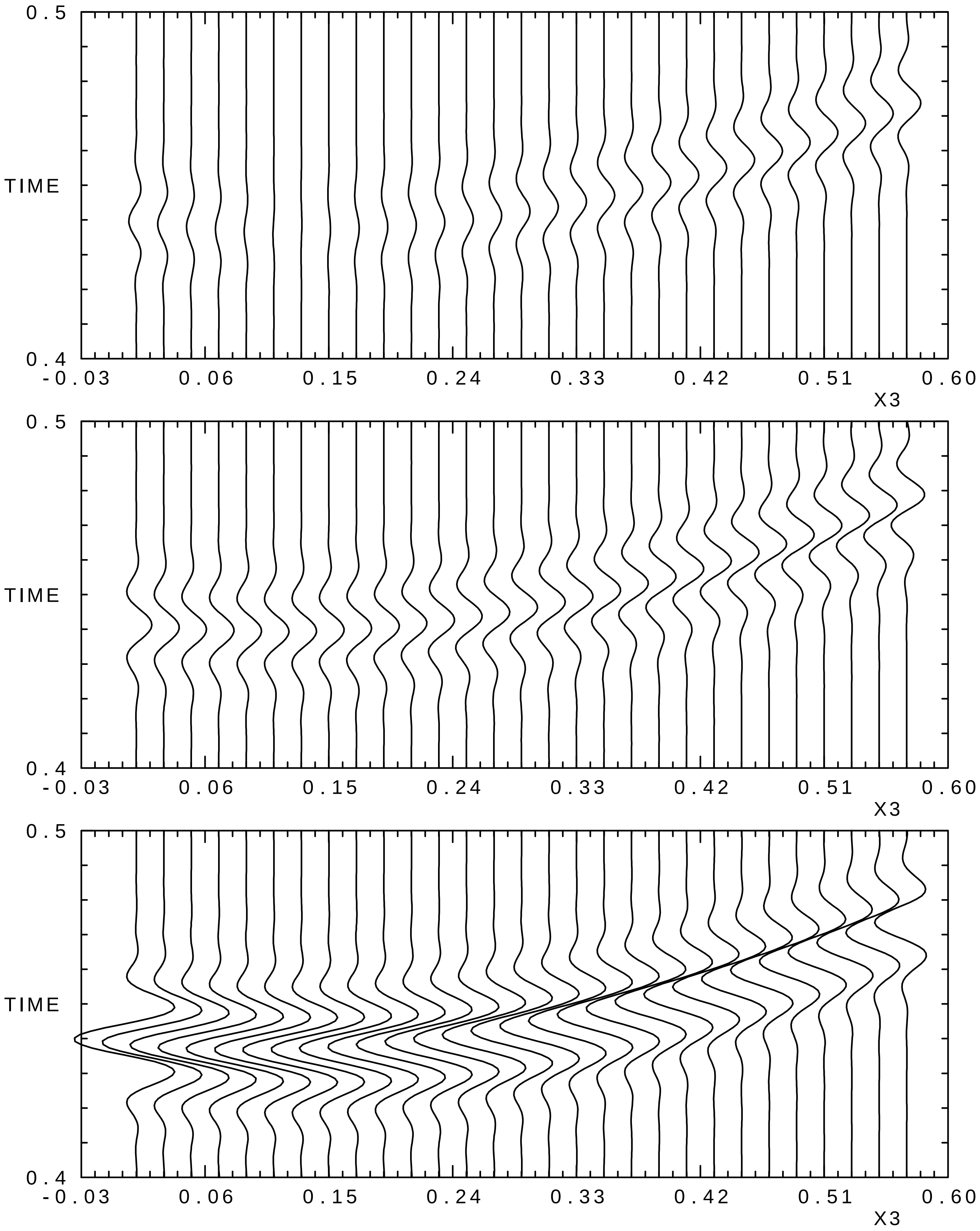

Figure 4. Anisotropic–ray–theory seismograms in model QIH. From top to bottom: the first (radial) component, the second (transverse) component, the third (vertical) component.

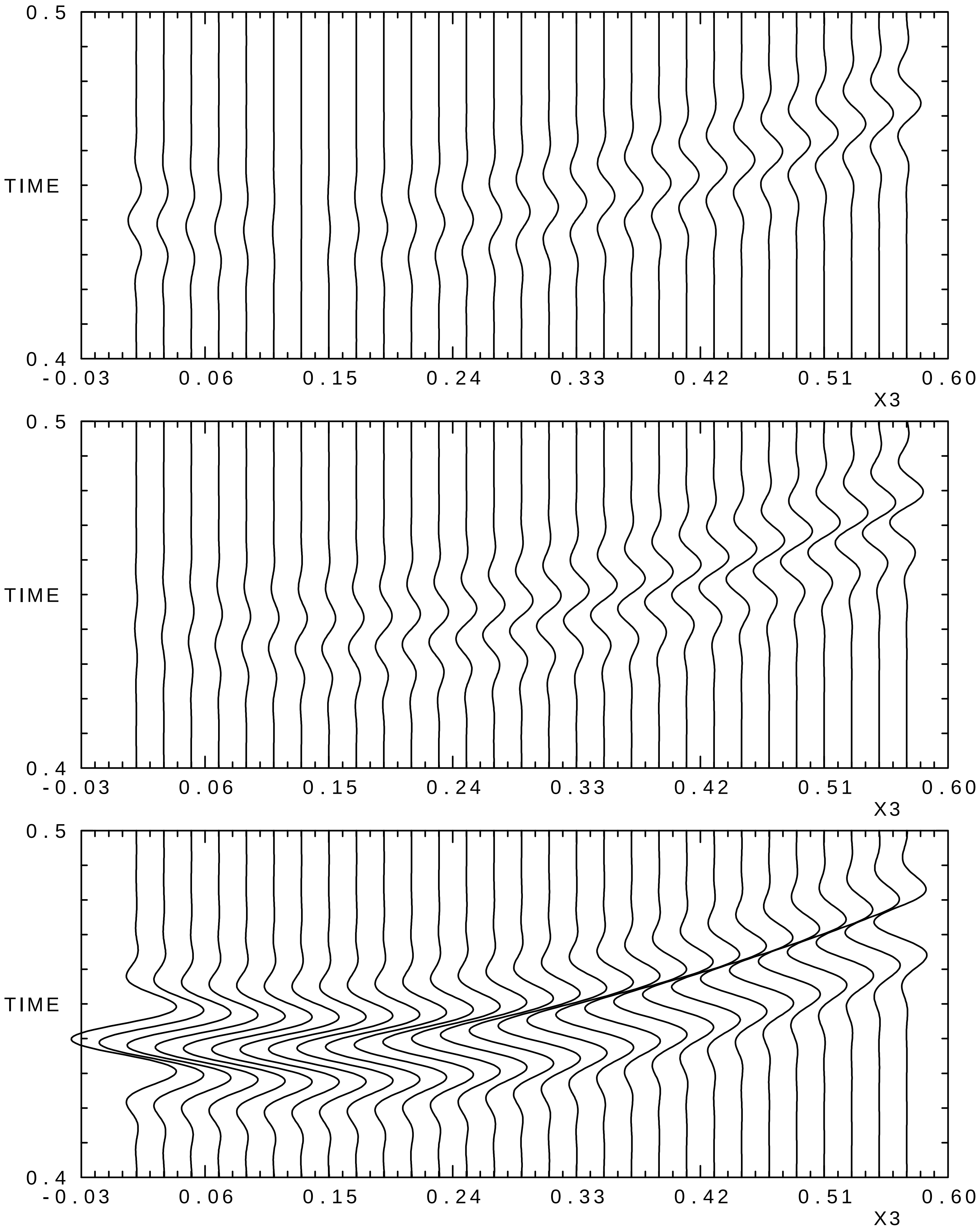

Figure 5. Coupling–ray–theory seismograms in model QIH. From top to bottom: the first (radial) component, the second (transverse) component, the third (vertical) component. Compare the second (transverse) component with Figures 3 and 4.

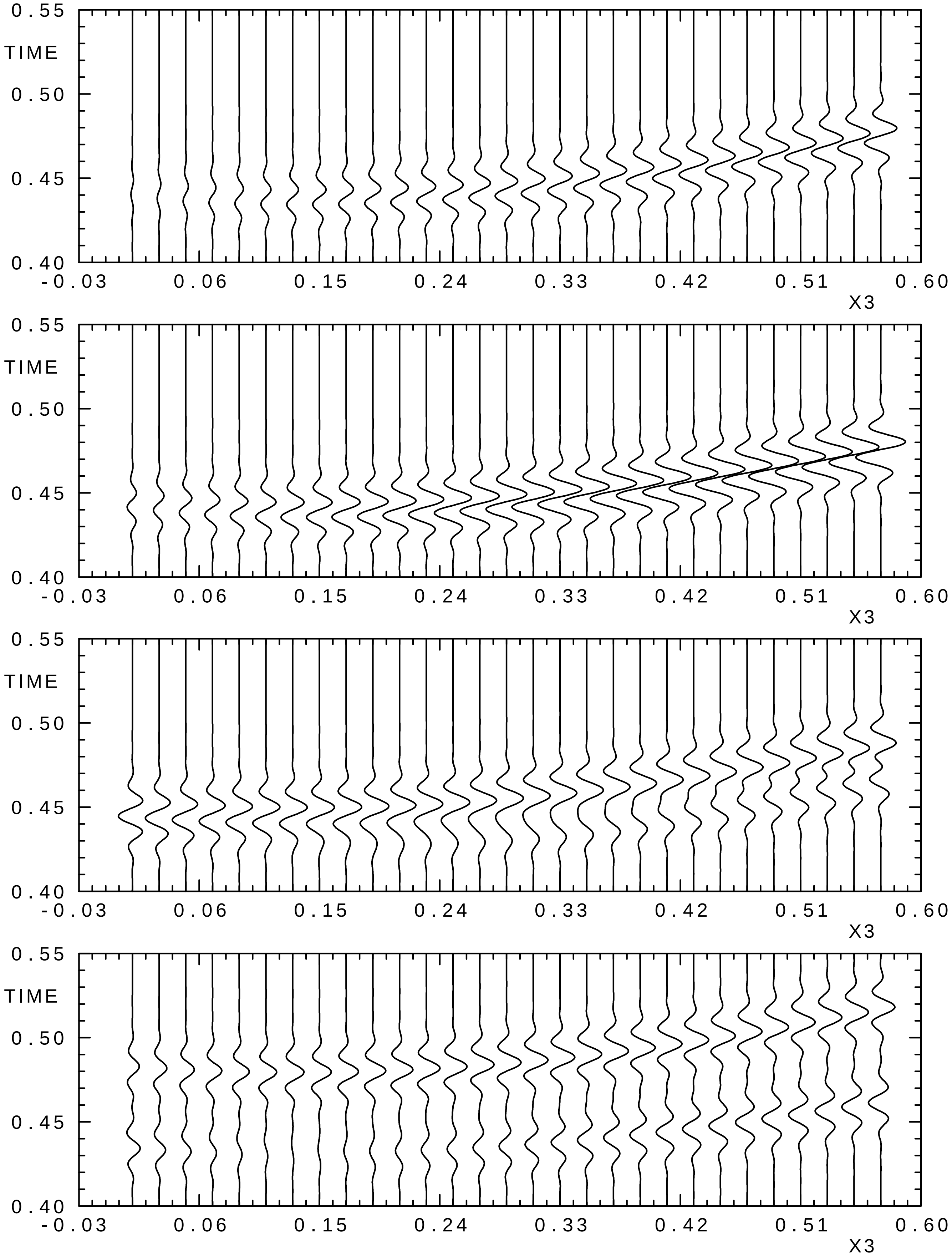

Figure 6. Coupling–ray–theory seismograms in models QIH, QI, QI2 and QI4 (from top to bottom). Only the second (transverse) component is shown. This component vanishes in the reference isotropic model QI0 (Figure 3). See the change of polarization indicated by clear increment of transverse amplitudes in the two upper models, and the clear development of S–wave splitting in the two bottom models.

Isotropic–ray–theory, coupling–ray–theory, and anisotropic–ray–theory seismograms in model QIH are compared in Figures 3, 4 and 5. The most pronounced differences can be observed in polarization. They are clearly visible on the second (transverse) component. A small time shift of the isotropic–ray–theory seismograms with respect to the anisotropic–ray–theory and coupling–ray–theory seismograms could be corrected by a better selection of the reference isotropic model.

The second (transverse) components of the coupling–ray–theory seismograms in all 4 anisotropic models QIH, QI, QI2 and QI4 are compared in Figure 6. For weak anisotropy, the change of polarization with increasing anisotropy is indicated by a clear increment of the transverse amplitudes in the two upper models. The clear development of S–wave splitting, if anisotropy is increased further, can be observed in the two bottom models.

Acknowledgements

The research has been supported by the Grant Agency of the Czech Republic under Contract 205/07/0032, by the Ministry of Education of the Czech Republic within research project MSM0021620860, by the European Commission under Contract MTKI-CT-2004-517242 (project IMAGES), and by the members of the consortium "Seismic Waves in Complex 3–D Structures" (see "http://sw3d.mff.cuni.cz").

References

Bulant, P. & Klimeš, L. (2002): Numerical algorithm of the coupling ray theory in weakly anisotropic media. *Pure appl. Geophys.*, **159**, 1419–1435.

Coates, R.T. & Chapman, C.H. (1990): Quasi–shear wave coupling in weakly anisotropic 3-D media. *Geophys. J. int.*, **103**, 301–320.

Klimeš, L. & Bulant, P. (2004): Errors due to the common ray approximations of the coupling ray theory. *Stud. geophys. geod.*, **48**, 117–142.

Klimeš, L. & Bulant, P. (2006): Errors due to the anisotropic–common–ray approximation of the coupling ray theory. *Stud. geophys. geod.*, **50**, 463-477.

Pšenčík, I. (1998): Green's functions for inhomogeneous weakly anisotropic media. *Geophys. J. int.*, **135**, 279–288.

Pšenčík, I. & Dellinger, J. (2001): Quasi–shear waves in inhomogeneous weakly anisotropic media by the quasi–isotropic approach: A model study. *Geophysics*, **66**, 308–319.

Thomson, C.J., Kendall, J-M. & Guest, W.S. (1992): Geometrical theory of shear–wave splitting: corrections to ray theory for interference in isotropic/anisotropic transitions. *Geophys. J. int.*, **108**, 339–363.